EVIDENCE OF DISTURBANCE IN THE ^{26}Al-^{26}Mg SYSTEMATICS OF THE EFREMOVKA E60 CAI: IMPLICATIONS FOR THE HIGH-RESOLUTION CHRONOLOGY OF THE EARLY SOLAR SYSTEM.

M. Wadhwa[1], P. E. Janney[1], and A. N. Krot[2]. [1]Center for Meteorite Studies, School of Earth and Space Exploration, Arizona State University, Tempe, AZ 85287, USA [2]Hawai'i Institute of Geophysics and Planetology, School of Ocean and Earth Science and Technology, University of Hawai'i at Mānoa, Honolulu, HI 96822, USA.

Introduction: The high-resolution ^{26}Al-^{26}Mg extinct chronometer ($t_{1/2}$ = 0.72 Myr) has been applied extensively towards constraining the chronology of the early Solar System. In particular, there have been many investigations of the ^{26}Al-^{26}Mg systematics in the calcium-aluminum-rich inclusions (CAIs), which has been used to infer the age of the Solar System since these objects represent the earliest-formed solids in the solar nebula (e.g., [1-5]). However, this chronometer can only provide relative time constraints and has to be anchored to the high-resolution Pb-Pb chronometer to obtain absolute ages. There are relatively few CAIs for which both internal Al-Mg and Pb-Pb systematics have been determined. One such CAI is E60 from the Efremovka reduced CV3 chondrite, for which an internal Al-Mg isochron corresponding to a ^{26}Al/^{27}Al ratio of $4.63 \pm 0.44 \times 10^{-5}$ has been determined [6] and a highly precise Pb-Pb age of 4567.11 ± 0.16 Ma has also been reported [7]. However, recent investigations (e.g., [8]) have brought to light discrepancies between the Pb-Pb ages for CAIs and the Al-Mg systematics in these objects. Additionally, Al-Mg systematics in the angrites D'Orbigny and Sahara 99555 anchored to the E60 CAI yield ages that are ~2 Myr younger than the Pb-Pb ages for these achondrites ([9] and references therein). Therefore, with the goal of assessing the suitability of E60 CAI as a time anchor for the ^{26}Al-^{26}Mg system, we have performed high-precision laser ablation multicollector inductively coupled plasma mass spectrometer (LA-MC-ICPMS) analyses of minerals in rim and the interior of this inclusion.

Analytical Methods: The mineralogy and petrography of a polished thick slice of the Efremovka E60 CAI were studied using a Cameca SX-50 electron microprobe and a JEOL JSM-5900LV scanning electron microscope (SEM) equipped with a Thermo Electron energy dispersive spectrometer. Magnesium isotopes were measured with a Thermo-Finnigan Neptune MC- ICPMS instrument and a Photon Machines fast excimer laser ablation system (producing 193 nm wavelength and 4 ns pulse length) at Arizona State University using methods similar (unless noted here) to those described in [10]. Analyses were conducted in medium resolution mode to resolve any interferences on the Mg masses. Individual measurements typically consisted of 25 integration cycles, each of 8.4 sec duration. The laser spot size was 40-90 μm, with a repeat rate of 4 Hz and a laser energy density of roughly 2.8 J/cm^2. Signal intensity for ^{24}Mg ranged from 0.5 to 3.0×10^{-11} A. All measurements employed sample-standard bracketing, using isotopically well-characterized synthetic glasses from evaporation experiments having CAI-like compositions [11]. Standard glass compositions were chosen that approached the compositions of the analyzed phases. Based on repeated measurements of these glasses, typical external reproducibilities (2σ) for the ^{27}Al/^{24}Mg ratios and the δ^{26}Mg* values (defined as the non mass-dependent deviations in the ^{26}Mg/^{24}Mg ratio relative to the DSM3 standard) are ±5% and ±0.15‰, respectively.

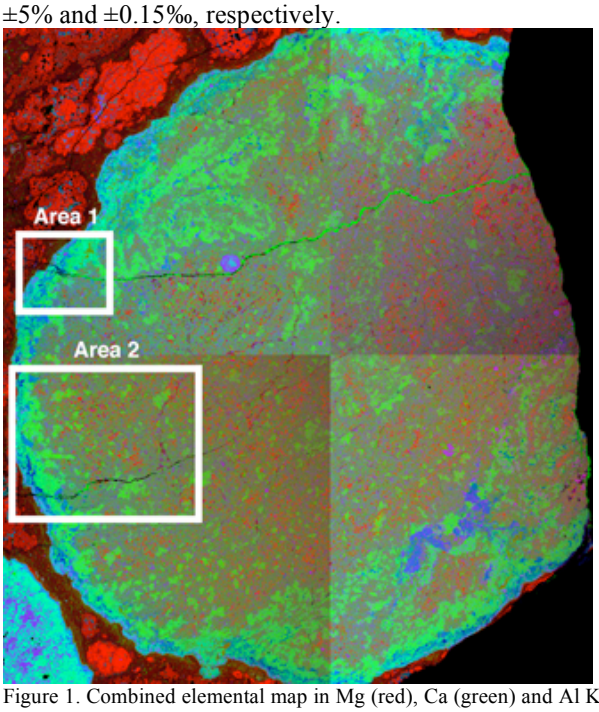

Figure 1. Combined elemental map in Mg (red), Ca (green) and Al Kα (blue) X-rays of the Efremovka E60 CAI. forsterite is red; melilite is light-green; diopside is dark-green; anorthite is blue; nepheline is dark-blue; spinel is purple. The CAI is ~1.1 mm in the longest dimension. LA-ICPMS analyses were conducted on mineral phases in the areas outlined in white; Figs. 2 and 3 show these areas in greater detail.

Results and Discussion: Figures 1-3 show the locations of the spots analyzed in the E60 CAI by LA-MC-ICPMS. Analyses were made on the diopside-rich rim (Rim-1) and on diopside in the interior of the CAI (Diopsides I-1 and I-2) (Fig. 2). Measurements were also performed on melilites in the rim (Melilites R-1, R-2 and R-3) and in the interior (Melilites I-1, I-2 and I-3), and on anorthites in the rim (Anorthites 2-1, 2-2a and 2-2b). All of the analyzed phases showed resolvable excesses in radiogenic ^{26}Mg (^{26}Mg*) (Fig. 4).

As shown in Fig. 4, with the exception of the three melilite rim analyses, all of the analyzed phases lie along

an isochron with a slope corresponding to a $^{26}Al/^{27}Al$ ratio of ~3 × 10^{-5}. The disturbance of the ^{26}Al-^{26}Mg systematics in E60 is evident from the lower than canonical value to the slope of this isochron, the positive initial δMg* value of 0.21 ± 0.07, and the three melilite rim analyses that fall to the left of this isochron (Fig. 4).

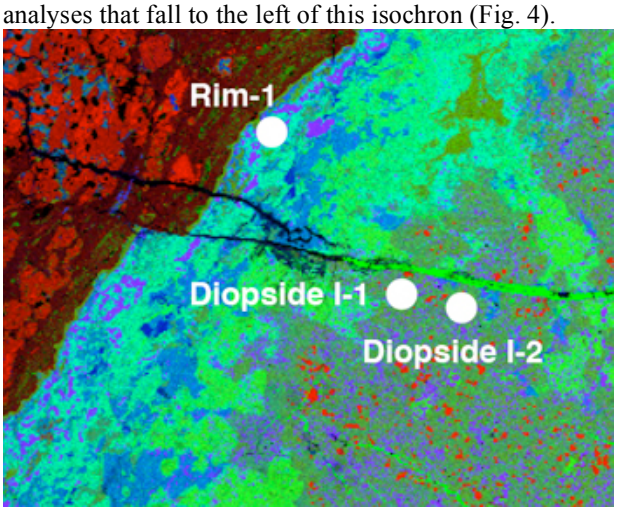

Figure 2. Combined elemental map in Mg (red), Ca (green) and Al Kα (blue) X-rays of area 1 (see Fig. 1) of E60. Positions of the laser ablation spots (each ~40 μm in diameter) are shown as the white circles. "Rim-1" is composed mostly of diopside in rim, but has some overlap with melilite and spinel. Two additional spots were analyzed on diopside in the interior of the CAI (Diopside I-1 and Diopside I-2).

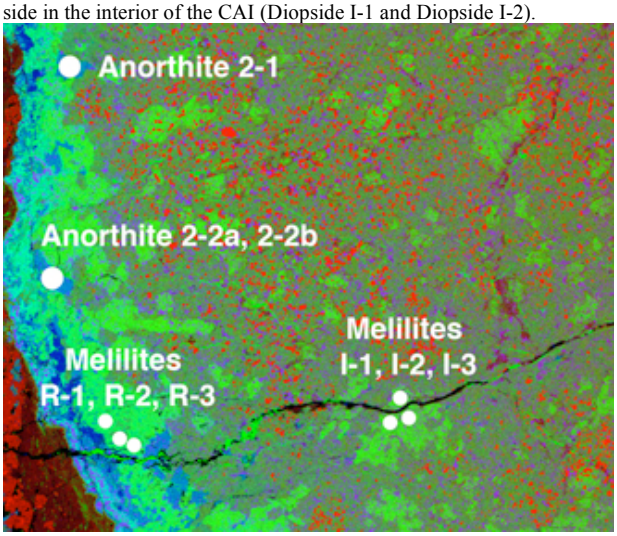

Figure 3. Combined elemental map in Mg (red), Ca (green) and Al Kα (blue) X-rays of area 2 (see Fig. 1) of E60. Locations of the laser ablation spots (~90 μm in diameter on anorthites and ~40 μm on melilites) are shown as the white circles. Only one spot location is noted for "Anorthite 2-2a" and "Anorthite 2-2b" as these represent analyses on the same spot.

The $^{26}Al/^{27}Al$ ratio corresponding to the isochron shown in Fig. 4 is slightly lower than the value determined previously by ion microprobe analyses of this CAI [6]. The latter was primarily constrained by two anorthites with high $^{27}Al/^{24}Mg$ ratios (up to ~144), which were the only phases analyzed by [6] that showed resolvable excesses in $^{26}Mg^*$. It is possible that the apparent inconsistency between the results of this study and those reported by [6] could be due to some heterogeneity in the extent of isotopic disturbance in the E60 CAI; this is not unlikely given that Efremovka has experienced extensive shock and some thermal metamorphism [12, 13]. We plan to assess this possibility with further analyses of other areas in this inclusion.

If it is assumed that the $^{26}Al/^{27}Al$ ratio defined by the isochron shown in Fig. 4 corresponds to the time when the Pb-Pb age for E60 (4567.1 ± 0.2 Ma; [7]) was also reset, the true formation age of this inclusion (when the $^{26}Al/^{27}Al$ ratio was ~5 × 10^{-5}) could be up to ~1 Myr older. In conclusion, until further analyses can be made to more rigorously assess the extent of isotopic disturbance in E60, the high-precision ^{26}Al-^{26}Mg systematics presented here for this inclusion suggest that it may not be an appropriate time anchor for the short-lived ^{26}Al-^{26}Mg chronometer.

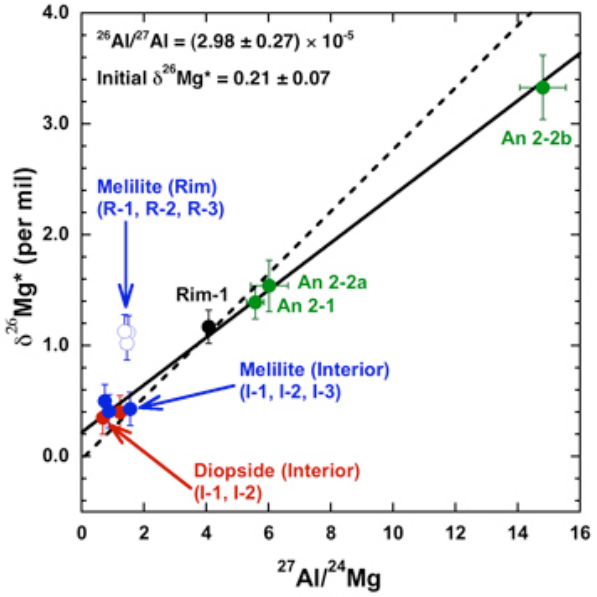

Figure 4. ^{26}Al-^{26}Mg systematics in the Efremovka E60 CAI: rim diopside (solid black circle), interior diopside (solid red circles), rim melilite (open blue circles), interior melilite (solid blue circles), and anorthite (solid green circles). The solid line is the regression through all the data points except for the three melilite rim analyses (R-1, R-2, R-3) and corresponds to $^{26}Al/^{27}Al = 2.98 \pm 0.27 \times 10^{-5}$ (MSWD = 1.1). For reference, the dashed line, constrained to pass through the bulk chondritic data point (Al/Mg ~0.10 and δMg* ~0), corresponds to the canonical $^{26}Al/^{27}Al$ ratio of 5 × 10^{-5}.

References: [1] MacPherson G. J. et al. (1995) *MAPS 30*, 365-386. [2] Bizzarro M. et al. (2004) *Nature 431*, 275-278. [3] Young E. D. et al. (2005) *Science 308*, 223-227. [4] Thrane K. et al. (2006) *ApJ* 646, L159-L162; [5] Jacobsen B. et al. (2008) *EPSL 272*, 353-364. [6] Amelin Y. et al. (2002) *Science 297*, 1678-1683. [7] Amelin Y. et al. (2006) 38th *LPSC*, Abstract #1970. [8] Bouvier A. and Wadhwa M. (2009) *40th LPSC*, submitted. [9] Spivak-Birndorf et al. (2009) *GCA*, in revision. [10] MacPherson G. J. et al. (2008) *ApJ*, in press. [11] Richter F. M. et al. (2007) *GCA 71*, 5544-5564. [12] Scott E. R. D et al. (1992) *GCA 56*, 4281-4293. [13] Bonal L. et al. (2006) *GCA 70*, 1849-1863.